



Topography and Tree Species Improve Estimates of Spatial Variation in Soil Greenhouse Gas Fluxes in a Subtropical Forest

Andrew W. Quebbeman,¹ Duncan N. L. Menge,¹ Jess Zimmerman,² and María Uriarte^{1*}

¹Department of Ecology, Evolution and Environmental Biology, Columbia University, New York, NY, USA; ²Department of Environmental Sciences, University of Puerto Rico, San Juan, Puerto Rico, USA

ABSTRACT

Subtropical and tropical forests account for over 50% of soil CO₂ production, 47% of N₂O fluxes of natural ecosystems, and act as both significant sources and sinks of atmospheric CH₄. However, ecosystem-scale estimates of these fluxes typically do not account for uncertainty that arises from environmental heterogeneity over small spatial scales. To assess the effects of small-scale environmental heterogeneity on GHG fluxes in a tropical forest ecosystem, we measured fluxes of CO₂, CH₄, and N₂O across a topographic gradient and at the base of different tree species. We then used Bayesian linear models together with maps of trees and topography to quantify spatial heterogeneity in ecosystem-scale estimates of GHG emissions. The relationship between GHG fluxes and species and topography varied for each gas type. CO₂ varied strongly by species but was only weakly related to topographic variation. In contrast, CH₄ and N₂O,

which are more strongly regulated by soil oxygen, had strong relationships with topography but did not vary across species. Assuming spatial homogeneity and average rainfall conditions, we estimated ecosystem soil CO₂ emissions to be 28.91 kg CO₂-C/ha/day, net CH₄ consumption of – 5.15 g CH₄-C/ha/day, and net N₂O emissions of 1.78 g N₂O-N/ha/day. Including variation caused by tree species decreased ecosystem-level estimates of CO₂ emissions by 8.03%, whereas including topographic variation decreased net CH₄ consumption by 12.98% and increased net N₂O emissions by 1.05%. This translates to a net decrease of 8.32% in estimated CO₂-equivalent emissions. Our findings show that ignoring small-scale environmental heterogeneity has implications for bottom-up estimates of GHG fluxes in tropical forests. Given the increasing availability of fine-scale topographic models, incorporating this source of variation in estimates of ecosystem soil GHG emissions could improve our understanding of the role tropical forests play in global GHG cycles.

Received 5 March 2021; accepted 19 June 2021;
published online 19 July 2021

Supplementary Information: The online version contains supplementary material available at <https://doi.org/10.1007/s10021-021-00677-x>.

Author contributions AQ, DM, and MU conceived the study. AQ performed the research, and AQ and MU analyzed data. JZ and MU collected tree data. AQ wrote the first draft, and all authors contributed to the final version.

*Corresponding author; e-mail: mu2126@columbia.edu

Key words: Tropical forests; Methane; Nitrous oxide; Carbon dioxide; Soil GHG fluxes; Puerto Rico; Spatial variation.

HIGHLIGHTS

- Model soil GHG fluxes accounting for topography and species distributions.
- Information about tree species affects estimates of ecosystem-scale soil CO₂ fluxes; information about topography that of CH₄ and N₂O.
- Incorporation of these factors enables landscape-level estimation of soil GHG fluxes.

INTRODUCTION

Tropical forests contribute disproportionately to global fluxes of carbon dioxide (CO₂), methane (CH₄), and nitrous oxide (N₂O) (Bouwman and others 1995; Curry 2007; Bond-Lamberty and Thomson 2010). At large scales, predictions of GHG fluxes rely on abiotic factors like climate and ecosystem type. However, environmental conditions within soils (for example, soil oxygen and moisture) can create variation at small spatial scales that is difficult to incorporate into large scale estimates of ecosystem soil GHG emissions (Bouwman and others 1995; Curry 2007; Groffman and others 2009; Bond-Lamberty and Thomson 2010). Because of the dynamic nature of the factors regulating these GHG fluxes, small discrepancies in our estimates can have significant effects on our predictions for the contribution of tropical forests to atmospheric greenhouse gases. Thus, studying small-scale variation in GHG fluxes and how this variation affects estimates of ecosystem soil GHG emissions is essential for improving our ability to accurately model global nutrient cycling and forecast climate (Bouwman and others 1995; Breuer and others 2000; Curry 2007).

Soil oxygen, moisture, and nutrients are three of the most important direct controls of soil GHG fluxes. Anoxic processes like methanogenesis and denitrification are often higher in wetter, low-oxygen soils (Silver and others 1999; Wood and Silver 2012), whereas autotrophic and heterotrophic soil respiration often peaks at intermediate soil moisture (Wood and others 2013; Schimel 2018). However, high soil moisture can also slow diffusion and decrease the rate of soil GHG fluxes at the soil surface (McSwiney and others 2001; Schimel 2018), sometimes leading to the highest fluxes at intermediate levels of soil moisture (Hall and others 2013; Wood and others 2013). Similarly, spatial variation in soil nutrient availability can create hotspots of biogeochemical activity and contribute to complex patterns of GHG fluxes.

Areas with abundant labile nitrogen often have higher rates of N₂O fluxes (Palta and others 2014), and soil nutrient availability can increase decomposition and soil CO₂ fluxes in tropical forests (Cleveland and Townsend 2006). Despite the well-characterized effects of soil oxygen, moisture, and nutrients on GHG fluxes (Silver and others 1999; Groffman and others 2009; Wood and others 2013; Palta and others 2014; Schimel 2018), it is often difficult to assess how small-scale environmental heterogeneity in these drivers influences estimation of ecosystem-scale GHG emissions.

One way to incorporate the direct controls of environmental heterogeneity on GHG fluxes into estimates of soil ecosystem GHG emissions is to use proxies for small-scale variation in soil oxygen, moisture, and nutrients. Topography is known to influence small-scale spatial patterns of soil oxygen and moisture (Silver and others 1999; Daws and others 2002; Wood and Silver 2012; Chadwick and Asner 2016) and is also relatively easy to quantify at large spatial scales with the advent of remote sensing technologies (for example, LiDAR). In wet forests (for example, rainforests), valleys have higher soil moisture than ridges and steep slopes and, as a result, often have lower soil oxygen, leading to soil redox conditions that favor higher production of CH₄ and consumption of N₂O (Silver and others 1999; Wood and Silver 2012; O'Connell and others 2018). Similarly, differences in tree distributions and characteristics can be useful for capturing small-scale spatial patterns of soil nutrient availability (Zinke 1962; Reed and others 2008; Keller and others 2013; Uriarte and others 2015; Waring and others 2015). Patchiness in tree locations, differences in abundance, and high interspecific variation in litter chemistry, all of which are common in tropical forests (Condit 2000; Hättenschwiler and others 2008), are often associated with spatial heterogeneity in soil nitrogen cycling (Osborne and others 2017) and other soil macronutrients (Keller and others 2013; Uriarte and others 2015; Waring and others 2015). Thus, using topography as a proxy for spatial variation in soil oxygen and moisture and tree species as proxies for patchiness in soil nutrients may allow us to incorporate small-scale environmental heterogeneity into ecosystem-scale GHG estimates.

Although the effects of topography and tree species on the soil environment are common, they are not ubiquitous, and sometimes they interact in complex ways (Powers and others 2004; Wood and Silver 2012; Hall and others 2013). The relationship between tree species and soil nutrients may be weak in tropical forests due to high species diversity

and overlapping canopies (Powers and others 2004; Waring and others 2015) or obscured by the effects of intrinsic soil characteristics such as soil moisture (Engelbrecht and others 2007) and soil nutrients (John and others 2007) on tree species' distributions. Additionally, tree species traits such as canopy structure can affect stemflow and throughfall and influence patterns of soil moisture and oxygen that may be independent of topography (Holwerda and others 2006; Heartsill-Scalley and others 2007). Topography can also influence patterns of soil nutrient availability by altering leaf litter accumulation and the movement of soil nutrients (Dwyer and Merriam 1981; Johnston 1992; Tateno and Takeda 2003; Osborne and others 2017). Based on the confounding effects of tree species and topography on the soil environment, the relative importance of these proximate drivers may vary for each GHG. By quantifying the extent to which tree species or topographic position can explain variation in GHG fluxes related to soil environmental heterogeneity, we can use these easier to measure proximate drivers of soil environmental variation (that is, topography and tree species) to incorporate small-scale spatial variation in GHG fluxes into estimates of soil ecosystem GHG emissions.

Here we use data from the 16-ha permanent mapped Luquillo Forest Dynamics Plot (LFDP) in Puerto Rico (18°20'N, 65°49'W) to quantify differences in GHG fluxes among topographic positions and five dominant tree species, two potential drivers of small-scale variation in GHG fluxes. We then use this information to assess how ecosystem-scale estimates of GHG emissions change with the inclusion of species-specific and topographic variation. Tree species' distributions and topography within the LFDP are well characterized (Thompson and others 2002), enabling us to determine the relationship between GHG fluxes and these proximate drivers of environmental heterogeneity. Additionally, the relatively low tree species diversity in the LFDP compared to mainland tropical forests (Condit 2000) make this site ideal for examining the effects of scaling up small-scale measurements of GHG fluxes to estimate ecosystem-scale emissions.

METHODS

To assess how environmental heterogeneity affects ecosystem estimates of GHG emissions, we measured CO₂, CH₄, and N₂O fluxes from soils at the base of individual trees from five focal tree species along a topographic gradient. We tested for differences in GHG fluxes by tree species and topography

by fitting linear Bayesian models to data for each of three GHG gas fluxes: CO₂, CH₄, and N₂O. To quantify how variation by species and topography influenced estimates of ecosystem-scale GHG emissions, we used the model coefficients along with data on topography and species distributions across the plot to estimate ecosystem-scale fluxes of CO₂, CH₄, and N₂O for the entire 16-hectare LFDP.

Study Site

Soil GHG fluxes were measured in the Luquillo Forest Dynamics Plot (LFDP) in the Luquillo Experimental Forest in northeastern Puerto Rico. The LFDP is a 16-hectare permanent, mapped forest plot established in 1990. The forest is classified as a subtropical wet forest in the Holdridge life zone system and the site average annual rainfall of 3,500 mm per year; mean annual temperature is 26 °C with little variability (Ewel and Whitmore 1973). Mean elevation of the LFDP is 350 m a.s.l.

Since 1990, all stems in the LFDP with a diameter greater than 1 cm at 1.30 m height (DBH) have been mapped, identified to species, and measured following a modified Center for Tropical Forest Science protocol (Condit 1998; Thompson and others 2002). Approximately every five years, trees are re-measured and their status is assessed. New stems are added as they appear. As of 2016, our five focal species (*Casearia arborea*, *Dacryodes excelsa*, *Inga laurina*, *Manilkara bidentata*, and *Prestoea acuminata*) represented the five most abundant species in the LFDP and accounted for 46% of all stems at least 1 cm DBH, 68% of stems with a DBH at least 10 cm, and 53% of basal area in the LFDP (Supp. Table 1).

Topography of the LFDP was quantified from a high-resolution digital elevation model (DEM) derived from a LiDAR flyover of the forest in 2011 (Wolf and others 2016). We calculated a continuous measure of slope and concavity (that is, ridges vs. valleys) within the LFDP by fitting a six-term polynomial over a moving window with a radius of r to the DEM (Hurst and others 2012). The optimal r values for concavity and slope were determined for each GHG flux by maximizing the likelihood of the data given a model with only concavity and slope as covariates (Supp. Table 2). Positive values of concavity correspond with valleys and negative values represent ridges.

Gas Flux Sampling

Fluxes of CO₂, CH₄, and N₂O were measured from the soil at the base of 24 individuals of each of the five focal species (120 trees total). Individual trees

were randomly chosen using the 2016 LFDP census data after stratifying for species and topographic position (that is, concavity). To ensure individuals for each species represented the full range of concavity in the LFDP, we divided each species pool into 4 bins based on their concavity ($[-0.06$ to $-0.02]$, $[-0.02$ to $0]$, $[0$ to $0.02]$, and $[0.02$ to $0.05]$) and randomly selected six trees of each species from each bin, yielding a total of 24 trees per species for a total of 120 trees. For individuals selected in locations where GHG flux measurements were not possible, (that is, rocky outcrops), a nearby individual of the same species was selected. Fluxes were measured twice for each tree between May 29 and July 12, 2017. We measured all trees first and then re-measured the trees in the same order. The average time elapsed between measurements was 26 days, with a minimum of 20 and a maximum of 35 days.

To collect the gases, a 40-cm-diameter, 6.4-cm-height cylindrical chamber was placed on the surface of the soil, parallel to the slope, at 0.5 m from the base of each individual tree. A seal was created between the chamber edges and the soil surface by fitting robust plastic sheeting tightly around the base of the chamber and weighting the sheeting with heavy chains (Min and others 2021). At intervals of 0, 5, 15, and 25 min, 15-mL gas samples were withdrawn from the chambers through a septum in the top of the chamber and transferred to pre-evacuated 10-mL Restek vials fitted with robust Geo-Microbial Technologies septa. Air temperature (Ambient Weather WS-2063-W-P Temperature Monitor) and soil moisture (HydroSense II: 12 cm depth) were measured at the end of gas sampling. After sampling, septa were sealed with silicon sealant to maintain positive pressurization and all gas samples were transported back to Columbia University in New York for analysis.

The concentrations of CO_2 , CH_4 , and N_2O were analyzed using gas chromatography (a series of two, 2 m Haysep-D columns; SRI 8610C, SRI Instruments, Torrance, CA, USA) with a Nickel-63 electron capture detector for N_2O and a flame ionization detector equipped with a methanizer for CO_2 and CH_4 . The gas chromatograph was calibrated with custom-ordered analytical grade standards from Tech Air (White Plains, NY). Vials without positive pressure at the time of analysis were categorized as “leaky” and discarded. GHG fluxes were calculated from the quadratic change of the gas concentrations over time after considering the chamber volume and air temperature at the time of collection (Parkin and others 2012). Chamber flux measurements that had quadratic fits

with R^2 below 0.6 for CO_2 flux were removed. Negative fluxes represent net uptake into the soil, whereas positive values represent net soil emissions. All GHG flux measurements were discarded for trees with negative CO_2 flux estimates, which suggests an issue with the sampling chamber placement and seal. The final total number of usable soil GHG flux samples is provided in Supp. Table 3.

Statistical Analysis

Rainfall was highly variable during the sampling period (Supp Figure 1) and is a well-known driver of GHG emissions via its effects on soil moisture (Butterbach-Bahl and others 2004). Although we had measured soil moisture at the same time of GHG sample collection, our ability to capture spatial variation in soil moisture at the site using the HydroSense II probe is limited to extremely dry conditions (lower 5% daily precipitation quantile for observed historical precipitation (Uriarte and others 2018)) so we chose to use 48-h antecedent rainfall as a covariate in all models rather than soil moisture. Rainfall was standardized by subtracting the mean and dividing by the standard deviation for all observation. This formulation allows us to interpret parameters for species and topography as the effect of these covariates at average rainfall conditions.

To derive estimates for each of the CO_2 , CH_4 , and N_2O fluxes, we fit four models to the data (Table 1). The first model (M1) only had rainfall as a covariate and therefore provided an estimate of the average GHG flux across all our samples under average rainfall conditions; this represents a null model, as it implies no differences in GHG fluxes by species or topography. The second model (M2) allowed for differences in fluxes by species, and the third (M3) allowed for differences in fluxes by topography. The fourth model (M4) allowed flux estimates to vary by both species and topography. A normal likelihood distribution was used for CO_2 , CH_4 , and N_2O fluxes. Slope and concavity were standardized to facilitate model fit by subtracting the mean and dividing by the standard deviation. These four models allowed us to examine how well slope and concavity and proximity to focal tree species capture variation in measured GHG fluxes after accounting for rainfall variability.

Posterior distributions of parameters were estimated using Markov chain Monte Carlo (MCMC) methods using the *rjags* R package (Plummer 2011; R Core Team 2018). Three chains were computed for each parameter with uninformed, random ini-

Table 1. Model Type and Structure Used to Test the Relationship Between GHG Fluxes, Topography, and Trees.

M1: average flux (null model)	$Flux \sim \beta_0 + \beta_{rain} * rainfall + \epsilon$
M2: species-specific flux	$Flux \sim \beta_0 + \beta_i * species_i + \beta_{rain} * rainfall + \epsilon$
M3: topography-specific flux	$Flux \sim \beta_0 + \beta_{con} * concavity + \beta_{slope} * slope + \beta_{rain} * rainfall + \epsilon$
M4: species and topography-specific flux	$Flux \sim \beta_0 + \beta_i * species_i + \beta_{con} * concavity + \beta_{slope} * slope + \beta_{rain} * rainfall + \epsilon$

Species is included as a categorical factor, while topographical variables (concavity and slope) are continuous. In all models, the residuals (ϵ) are assumed to follow a normal distribution.

tial values. The first 5,000 iterations were discarded, and each chain ran for 10,000 iterations. Convergence was assessed by visually inspecting trace plots of chains. Finally, model fit was assessed using DIC scores; models with the lowest Deviance Information Criterion (DIC) scores were considered best fits (Spiegelhalter and others 2014). Significant effects of topography and species were determined using the 95% credible intervals for coefficient estimates. Goodness of fit (R^2) was calculated for best fit models.

Estimating Ecosystem Soil GHG Emissions

To incorporate small-scale spatial variation in GHG fluxes in our estimates of ecosystem soil GHG emissions, we assigned a GHG flux to each individual tree in the LFDP at the time of the 2016 census using coefficient estimates for each of the four models. These individual tree estimates used the species IDs and topography at each tree's location. For individuals not identified as one of the five focal species, we used the average extracted from M1. To incorporate uncertainty in coefficient estimates into our ecosystem-scale soil GHG estimates, we calculated ecosystem soil GHG emissions as a derived parameter (that is, by sampling the distribution of model parameters) within each model. This approach allowed us to estimate credible intervals for each ecosystem GHG estimate.

To compare the combined effect of model estimates on CO₂, CH₄, and N₂O fluxes, we used global warming potentials (using the standard 20 and 100 year equivalencies) to calculate a CO₂-equivalent ecosystem emission for each model (Solomon and others 2007). To calculate a CO₂-equivalent ecosystem emission, CH₄ fluxes were scaled by 72 (20 year) and 25 (100 year), N₂O fluxes were scaled by 289 (20 year) and 298 (100 year), and CO₂ fluxes were scaled by 1 (Solomon and others 2007). Total CO₂-equivalent estimates for each model were calculated as the sum of scaled CO₂, CH₄, and N₂O estimates.

To account for variation in individual tree estimates in our ecosystem soil GHG emissions, we scaled each individual tree's gas flux by a fraction of area of the LFDP using Dirichlet tessellation (*spatstat*: Baddeley and others 2015). The tessellation was calculated by dividing the area of the LFDP into polygons for each individual tree; the size of each polygon was influenced by the distance to nearest neighbors and scaled by tree size, such that, on average, each large tree accounts for a larger fraction of LFDP area than each small tree. Ecosystem GHG emission estimates were then calculated by summing GHG fluxes across the estimates for all individual trees. Ecosystem-scale GHG flux estimates were calculated in two ways: including all trees above 1 cm DBH.

To assess the effect of species-specific and topographic variation on ecosystem CO₂, CH₄, and N₂O emission estimates, we compared the ecosystem-scale GHG fluxes from M2, M3, and M4 to our null model (M1). Differences between model ecosystem emission estimates were significant if 95% credible intervals did not overlap.

RESULTS

Overview

We found a significant difference in soil CO₂ production by species and a positive relationship with concavity for both net CH₄ fluxes and N₂O fluxes. High antecedent rainfall increased CO₂ fluxes but did not affect soil CH₄ or N₂O fluxes. Using model results to estimate ecosystem soil GHG emissions under average rainfall conditions at the scale of the LFDP, we found that including species generally decreased estimates of ecosystem CO₂ production by 8.02% while including topography decreased CH₄ consumption by 12.98% and increased estimates of N₂O production by 1.05%.

Table 2. Penalized Δ DIC Scores for Models for Each Gas Type and R^2 of Best Models.

Model	CO ₂	CH ₄	N ₂ O
M1 (Null)	17.3	3.9	7.9
M2 (Species)	0	7.5	14.7
M3 (Topography)	13.3	0	0
M4 (Both)	2.9	2.1	6.8
R^2 of best model	23.07	11.4	11.3

A Δ DIC of zero indicates the best model fit. Generally, Δ DIC scores < 4 are not significantly different (Spiegelhalter and others 2014). Model descriptions same as Table 1.

GHG Fluxes Across Species and Topography

The relationship between GHG fluxes and species and topography varied for each gas type. CO₂ varied strongly by species but was only weakly related to topographic variation. In contrast, CH₄ and N₂O, which are more strongly regulated by soil oxygen, had strong relationships with topography but did not vary across species. Overall, compared to the null model (M1), models including species were better fits for estimates of CO₂ and models including topography were better for estimates of CH₄ and N₂O (Table 2).

The null model (M1) estimated CO₂ fluxes as 2.89 g CO₂-C/m²/day (Figure 1, Supp. Table 4). When we allowed fluxes to vary by species (M2), we found that two species (*I. laurina* and *P. acuminata*) had lower CO₂ production compared to the other three species; CO₂ fluxes for these species were 2.42 and 2.13 g CO₂-C/m²/day, respectively (Figure 1). The coefficient estimates for species were similar between M2 and M4. The relationship between topography and CO₂ fluxes (M3) is not significant. The DIC values for these models also support the inclusion of species but not topography for estimating CO₂ (Table 2).

For soil CH₄ fluxes, the null model (M1) estimated net consumption of CH₄ of -0.51 mg CH₄-C/m²/day (Supp. Table 4). Including species differences (M2) in estimates of CH₄ indicated significant net consumption (flux values < 0) by soils under one tree species (*D. excelsa*) of -1.12 mg CH₄-C/m²/day. The remaining four species had 95% credible intervals overlapping zero, which suggests neither net consumption nor production of CH₄ by soils under these species. The relationship between topography and CH₄ fluxes (M3) was stronger than for species; we found net CH₄ production is higher in valleys compared to ridges (0.48 mg CH₄-C/m²/day per standard deviation in

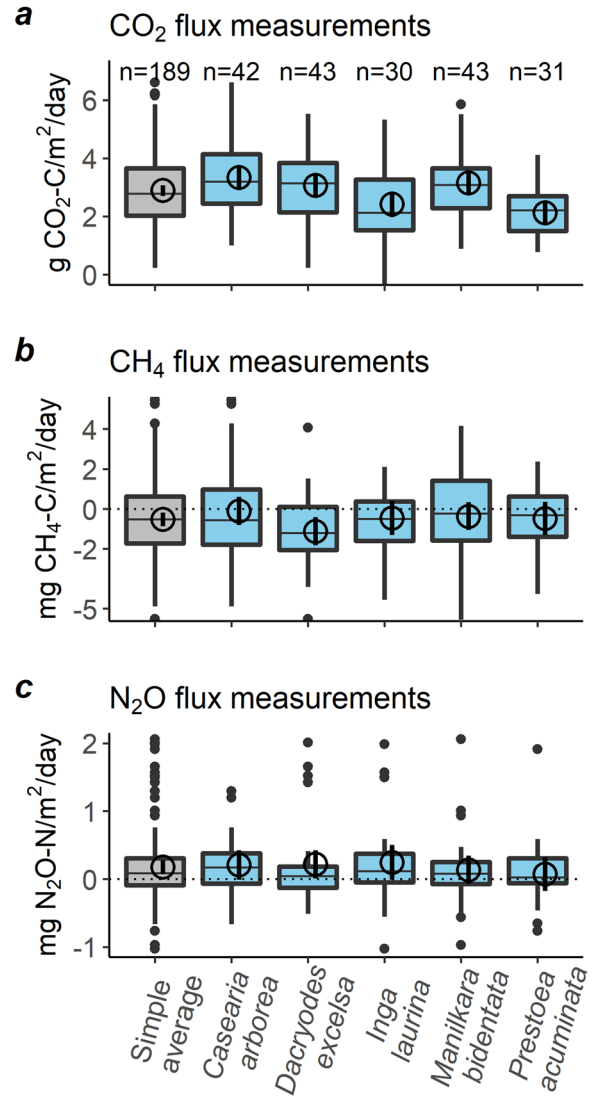


Figure 1. GHG fluxes by species. Boxplots show individual chamber flux data for the simple average (gray) and by species (blue). The large hollow point shows the model coefficient for the null estimate (M1) and species-specific estimates (M2). The bars centered on each hollow point show the 95% credible intervals for the null model and species-specific estimates.

concavity (Figure 2a, Supp. Table 4). The two models including topography had similar DIC values; however, M3 was the best fit (Table 2).

The null model (M1) estimated net production of N₂O at 0.18 mg N₂O-N/m²/day (Supp. Table 4). Like CH₄, there was no variation by species (M2) for estimates of N₂O fluxes; however, one species did show significant net N₂O production (*D. excelsa*; 0.22 mg N₂O-N/m²/day). N₂O production was lower in valleys compared to ridges and on steeper slopes (that is, estimated at -0.17 mg N₂O-N/m²/day per standard deviation in concavity: M3)

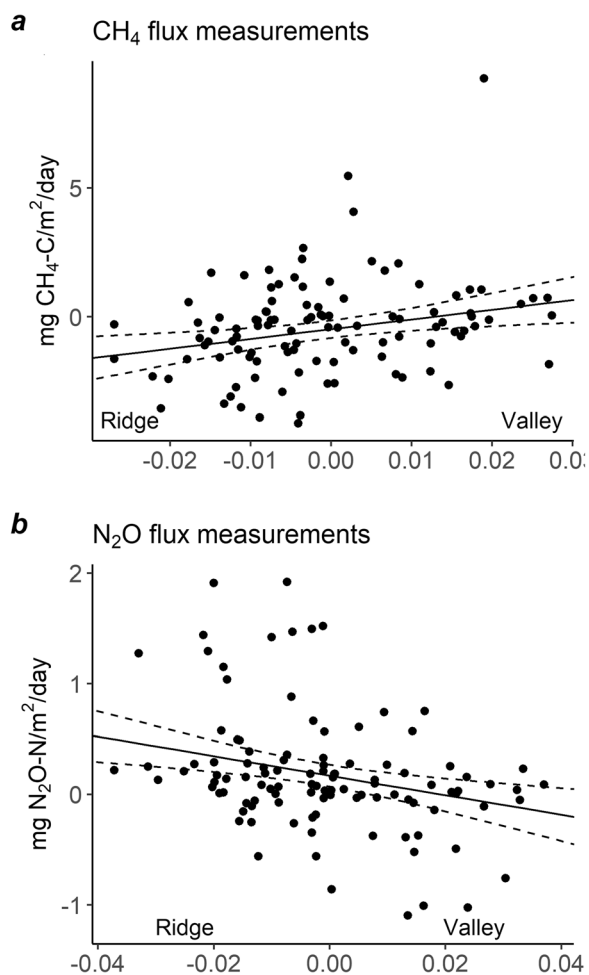


Figure 2. Linear relationships between concavity and CH₄ and N₂O. Data (black points) for CH₄ (panel a) and N₂O (panel b) fluxes by concavity. Solid black lines show the plotted model fits as functions of concavity (M3) with 95% credible intervals (dashed lines).

(Figure 2b, Supp. Table 4). Both models that included topography (M3 and M4) were better fits compared to M1 or M2, supporting the inclusion of topography in estimates of N₂O fluxes (Table 2).

Estimates of Ecosystem Soil GHG Emissions

Using the distribution of tree species and topography in the LFDP, we estimated spatial variation in ecosystem soil GHG emissions (Figure 3). We did not find significant differences between our simple average estimate of ecosystem soil GHG emissions and our model estimates; however, we discuss the direction of change caused by including small-scale variation in our ecosystem-scale estimates. Generally, scaling this small-scale variation using models that include species and topography (M2-M4) de-

creased estimates of ecosystem CO₂ and CH₄ fluxes and increased estimates of ecosystem N₂O fluxes compared to the null model (M1) (Supp. Table 5).

Our estimate of ecosystem CO₂ production that used all trees above 1 cm DBH decreased estimates by 8.08% and 7.83% (M2 and M4) compared to the null model (Figure 4), although these decreases were not statistically significant. Including species differences in our estimates decreased our estimate of soil CO₂ production from 28.9 kg CO₂-C/ha/day to 26.58 kg CO₂-C/ha/day (Supp. Table 5). In contrast, topography (M3) had little effect on CO₂ estimates compared to M1.

Differences in ecosystem estimates of CH₄ fluxes were non-significant across models, but there was a pattern of decrease in magnitude for models including species and topography. For all trees DBH above 1 cm, including species in estimates of soil CH₄ fluxes (M2) did not alter estimates of net CH₄ consumption (Figure 4). Including topography increased (less negative) CH₄ production estimates by 13% (M3) while the combined model for species and topography (M4) increased estimates of net CH₄ consumption by 11.37% from -5.09 to -5.67 g CH₄-C/ha/day (Supp. Table 5).

Estimates of soil N₂O production using all trees (DBH > 1 cm) decreased with the inclusion of species (M2) and topography (M3) compared to the null model; including species (M2) decreased estimates by 17.89% from 1.79 g to 1.47 g N₂O-N/ha/day (M2), whereas models including topography decreased estimates by 1.05% (M3) and 2.58% (M4) (Figure 4). Although these increases were not statistically significant, these results suggest small-scale variation in N₂O fluxes may increase estimates of ecosystem N₂O emissions.

Using global warming potentials to calculate the ecosystem-scale CO₂-equivalent ecosystem emissions, we found similar estimates between the 20- and 100-year equivalencies across model types. Including species decreased estimates of CO₂-equivalent ecosystem emissions by 8.32% (29.05 to 26.63 kg CO₂-C/ha/day; M2) for both the 20- and 100-year equivalencies compared to the null model (M1; Figure 5), but these differences were not significant. Including topography (M3) had a negligible (~1% increase) effect on CO₂-equivalent ecosystem emissions compared to the null model (M1).

DISCUSSION

Variation in soil GHG fluxes at small spatial scales contributes to uncertainty in estimates of ecosystem soil GHG emissions. While the direct controls

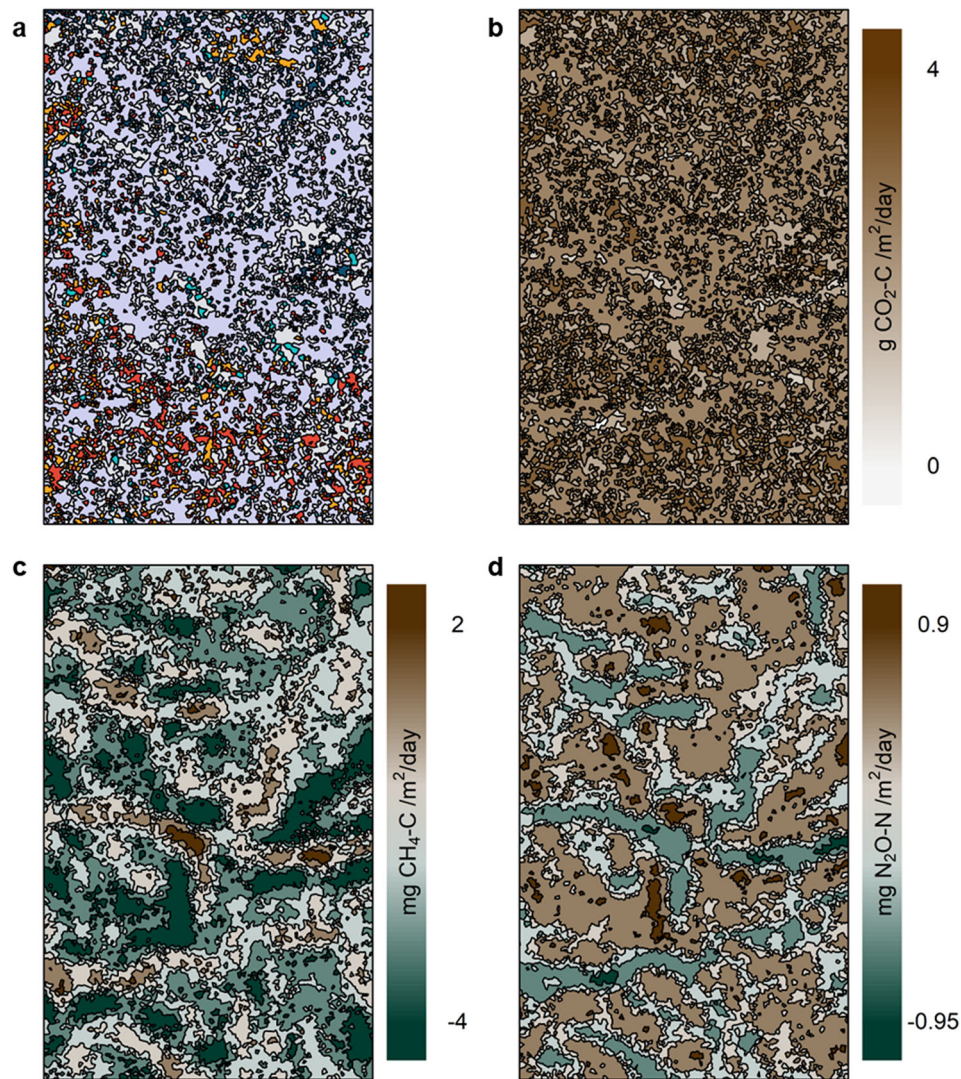


Figure 3. Maps of species and GHG fluxes in the Luquillo Forest Dynamics Plot. Tessellation area by species **a**, and individual tree estimates derived from model 4 for CO₂ **b**, CH₄ **c**, and N₂O **d**. Each color in Panel A is a separate species: *Casearia arborea* (dark blue), *Dacryodes excelsa* (red), *Inga laurina* (light blue), *Manilkara bidentata* (orange), *Prestoea acuminata* (lavender), and other (gray). Note that the positive (net production) ranges are different than the negative ranges (net consumption) for both CH₄ (C) and N₂O (D).

of GHG fluxes such as soil oxygen, moisture, and nutrients are well understood (Silver and others 1999; Groffman and others 2009; Wood and others 2013; Palta and others 2014; Schimel 2018), they are typically difficult to measure comprehensively at the larger spatial scales necessary to incorporate these factors into estimates of ecosystem-scale GHG fluxes. However, proxies that capture variation in these direct controls of soil GHG fluxes at larger spatial scales provide a way to assess the effects of small-scale environmental heterogeneity on ecosystem-scale estimates of GHG fluxes.

Topography and tree species are two comparatively easy to measure variables that are known to

influence soil oxygen and moisture (Silver and others 1999; Wood and Silver 2012), as well as soil nutrients (Reed and others 2008; Keller and others 2013; Uriarte and others 2015; Waring and others 2015). In this study, we first assessed if GHG fluxes varied across topography and tree species, as we hypothesized based on their expected effects on the soil environment. We then examined how estimates of ecosystem-scale GHG fluxes changed with the inclusion of variation in GHG fluxes related to topography and tree species. We found that the effects of species (for CO₂) and topography (for CH₄ and N₂O) were better predictors of gas fluxes than the null model. Given the importance of these

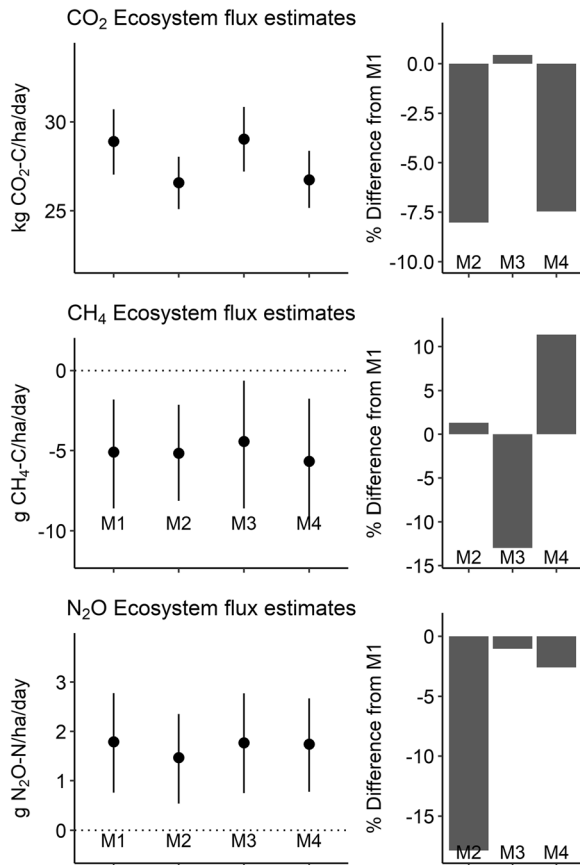


Figure 4. Ecosystem-scale GHG emissions (A, C, and E) and the percent change from M2-4 estimates compared to M1 (B, D, F) for CO₂ (A, B), CH₄ (C, D), and N₂O (E, F). X-axis separated by model results (M1: null model; M2: species-specific model; M3: topography model; M4: species and topography model). Error bars show 95% credible intervals.

proximate drivers of spatial variation, the ecosystem-scale estimates should diverge from the null model to the extent that the stratified sampling scheme over- or under-sampled tree species and topography relative to the underlying distribution of these variables across the LFDP.

Overall, we found that estimates of CO₂ fluxes varied more strongly by species than topography. The palm *P. acuminata* had lower CO₂ efflux and a tendency toward lower net N₂O efflux compared to other species. Palms are generally found in locally wet soils (Muscarella and others 2016, 2020), and high soil moisture can decrease rates of gas diffusion in soils (McSwiney and others 2001; Schimel 2018) and facilitate net N₂O consumption (Schlesinger 2013). Incorporating the relationship between palms and soil environmental heterogeneity could have large effects on estimated ecosystem soil GHG emissions, especially in the Neotropics where

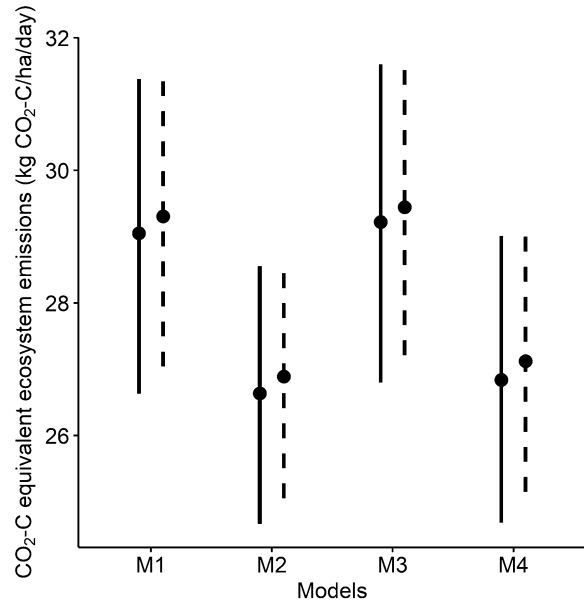


Figure 5. Total CO₂-equivalent of ecosystem soil GHG emissions. Values represent the 20-year (solid lines) and 100-year (dashed lines) CO₂-equivalent estimates (combined CO₂, CH₄, and N₂O fluxes) for each model: M1: null model; M2: species-specific model; M3: topography model; M4: species and topography model. Error bars show 95% credible intervals.

palms account for 6% of basal area and are five times more abundant compared to Paleotropical forests (Muscarella and others 2020).

In our study, spatial variation in CH₄ and N₂O fluxes was more strongly correlated with topography compared to CO₂ fluxes. Several studies have found that topography is often a useful measure of spatial variation in CO₂ (Epron and others 2006; Martin and Bolstad 2009), CH₄ (Kaiser and others 2018), and N₂O fluxes (McSwiney and others 2001). Other studies have observed weak or no relationships between topography and GHG fluxes (Wolf and others 2012; Courtois and others 2018); however, these studies did find that GHG fluxes were correlated with soil moisture and substrate availability independent of topography (Wolf and others 2012; Courtois and others 2018). Although we did not explicitly link topography to soil environmental conditions in our study, there is evidence that even at sites with low topographic variation (Martin and Bolstad 2009) or where the relationship between soil moisture and soil oxygen is weak (Kaiser and others 2018), topography can be useful as a proximate measure of small-scale spatial variation in GHG fluxes. In our study, the findings that valleys tended more toward CH₄ emissions make sense with a moisture-based

mechanism, as methanogenesis is an anoxic process (Silver and others 1999; Wood and Silver 2012). Similarly, the tendency for lower N_2O production and some N_2O consumption in valleys also fits with a moisture-based mechanism. Although denitrification is an anoxic process, it tends to go to completion (N_2 production rather than N_2O production) at high soil moisture (Davidson and others, 2000). Furthermore, N_2O consumption is more common in wet soils (Schlesinger 2013), likely because denitrification is favored in wet soils and atmospheric N_2O is available as an electron acceptor even after nitrate and nitrite have been reduced.

Although our study found a negligible effect of including species and topography to estimate soil ecosystem GHG emissions, other studies have found that ignoring small-scale spatial variation in GHG fluxes can underestimate ecosystem emissions by an order of magnitude (Vidon and others 2015; Kaiser and others 2018). Generally, these underestimations occur because measurement averaging approaches tend to mute the rare and extremely high GHG flux observations (Vidon and others 2015; Kaiser and others 2018). One of the biggest effects we observed was an 8.3% (albeit non-significant) decrease in estimates of ecosystem CO_2 fluxes after including species effects. We attribute this result to the dominance of the palm species *P. acuminata* in the LFDP, which accounted for only 20% of sampled trees, but 25% of all trees and 49% of large trees (DBH > 10 cm) in the plot and had lower GHG fluxes. The negligible effect of including species and topographic variation, despite their effects on small-scale flux measurements, suggests that our sampling design may have accurately captured both species and topographic variation across the plot and sufficiently captured spatial variation in GHG fluxes.

Our estimate of ecosystem-scale CO_2 (26.59 to 28.92 kg $\text{CO}_2\text{-C}/\text{ha}/\text{day}$), CH_4 (− 4.52 to − 5.65 g $\text{CH}_4\text{-C}/\text{ha}/\text{day}$), and N_2O (1.46 to 1.79 g $\text{N}_2\text{O-N}/\text{ha}/\text{day}$) fluxes fall at the lower range of estimates of ecosystem fluxes of CO_2 (12 to 186 kg $\text{CO}_2\text{-C}/\text{ha}/\text{day}$), CH_4 (− 8.5 to − 1.1 g $\text{CH}_4\text{-C}/\text{ha}/\text{day}$), and N_2O (− 3.07 to 7.39 g $\text{N}_2\text{O-N}/\text{ha}/\text{day}$) in nearby forests (Wood and Silver 2012; Hall and others 2013; Wood and others 2013). Wood and Silver (2012) also incorporated stratified sampling across a topographic gradient (that is, ridge, slope, valley) which may explain the similarity between our estimates. Our results, along with other studies (Vidon and others 2015; Kaiser and others 2018), suggest that ensuring GHG flux sampling schemes capture the frequency distribution of environ-

mental conditions driving variation in GHG fluxes could help constrain estimates of GHG fluxes in tropical forests. Additionally, incorporating spatial variation in GHG fluxes related to tree species and topography into our estimates of ecosystem soil GHG emissions decreased estimates of the total CO_2 -equivalent emissions in this forest by 8.5%; this amounts to a decrease of 1.8–2.2 kg $\text{CO}_2\text{-C}/\text{ha}/\text{day}$ for estimated CO_2 -equivalent emissions for this forest.

Incorporating the effects of spatial variation across species and topography on estimates of ecosystem soil GHG emissions may be difficult to do at large scales, especially in forests with high species diversity and complex terrain. However, advances in detecting species or plant traits across landscapes using remotely sensed images (Cook and others 2013; Tang and others 2021) may help distinguish species and incorporate species-specific variation in GHG fluxes into our estimates of ecosystem soil GHG emissions. This tool may also be useful for predicting variation in the soil environment as plant traits can often reflect soil properties (John et al 2007; Osborne and others 2017).

Additionally, methods that allow us to map topography at large scales (for example, lidar) would allow us to constrain estimates of GHG emissions based on the relationship between topography and the abiotic controls on GHG fluxes in soils. Although these methods can be resource-prohibitive in many places, mapped forest inventory plots, such as the CTFS-ForestGEO and LTER networks, offer a more widespread alternative, allowing researchers to explicitly include species abundances and topography into scaled-up estimates of GHG emissions. Our results suggest that sources of spatial variation in soil GHG fluxes should be considered when designing sampling schemes, even in places where topographic variation and species abundances are unknown. This is especially true for forests, which are more common on slopes and other topographically complex terrain because of global deforestation in topographically flat areas (Sandel and Svenning 2013).

Maximum estimates of net CH_4 production can be larger than net consumption in this forest (Silver and others 1999; O'Connell and others 2018)—our largest net CH_4 efflux measurement (9.22 mg $\text{CH}_4\text{-C}/\text{m}^2/\text{day}$) was 2.2 times the largest value for net CH_4 consumption (− 4.14 mg $\text{CH}_4\text{-C}/\text{m}^2/\text{day}$). While sampling across environmental variation (that is, species and topography) allowed us to account for the distribution of the spatial variation in CH_4 fluxes, this method likely under-estimated the effect of “hot moments” CH_4 effluxes common in

this forest (Silver and others 1999; O'Connell and others 2018).

Changes in temperature, precipitation, and disturbance regimes anticipated under climate change scenarios are predicted to have significant effects on the soil environment, potentially altering the contribution of tropical forests to global GHG emissions (Erickson and Ayala 2004; Vargas 2012; O'Connell and others 2018). Hurricanes are known to increase short-term CO₂ and N₂O fluxes in tropical forests by changing soil nutrient inputs and outputs (Erickson and Ayala 2004; Vargas 2012), and this response is likely dependent on tree species traits and responses to hurricanes. In contrast, an increase in drought frequency is predicted to decrease soil respiration in general (Wood and Silver 2012; Bouskill and others 2016), although the decrease may be less pronounced or switch to an increase in water-saturated forest soils, including those in valleys (Cleveland and others 2010; Wood and Silver 2012; O'Connell and others 2018). This is consistent with our finding of a positive effect of antecedent rainfall on CO₂ fluxes. Although we did not find an effect of rainfall on CH₄ fluxes, drought can also have strong effects on soil oxygen and carbon substrate availability, causing soils to shift from CH₄ sources to sinks or sinks to sources as soils recover (O'Connell and others 2018). Additionally, shifts in plant community composition and water regimes under climate change drive soil GHG emissions in tropical forest ecosystems and predicting forest response to climate change requires understanding the spatial variation in GHG fluxes across these factors.

By explicitly studying spatial variation in GHG fluxes, studies like ours can help to better constrain the effect of climate change on tropical forests; however, understanding the effects of climate change requires consideration of both the spatial and temporal variation in the soil environment and GHG fluxes. N₂O fluxes can change rapidly following precipitation events and changes in soil oxygen availability (Liptzin and others 2011; Hall and others 2013). In contrast, CO₂ fluxes often exhibit low diel variation and instead vary over the timescale of several days to weeks, related to both 2-day antecedent precipitation patterns (Wood and others 2013) and soil carbon substrate availability (Hall and others 2013).

Although seasonal changes can cause dramatic shifts in soil GHG fluxes (Verchot and others 2000; Kiese and others 2003), the temporal patterns of GHG fluxes in aseasonal forests can often exhibit greater spatial variation than temporal variation (Liptzin and others 2011). Additionally, the extent

of temporal variation can change across spatial covariates—for example, measurements in a nearby site had higher temporal variation in CH₄ fluxes in valleys compared to ridges (O'Connell and others 2018). Although this study focuses on linking proximate drivers of spatial variation in the soil environment to variation in GHG fluxes, these spatially explicit environmental covariates may be useful for understanding sources of temporal variation related to soil oxygen and substrate availability.

Our study highlights the importance of ensuring that sampling design captures small-scale environmental variation driving GHG fluxes to ensure the accuracy of the contribution of tropical forests to global GHG estimates. In addition to improving estimates of soil GHG fluxes, including the relationships between topography and species with GHG fluxes allowed us to model the spatially heterogeneous pattern of GHG fluxes across the landscape. By understanding the effects of these environmental factors on GHG fluxes, we can improve our predictions for how ecosystem soil GHG emissions may change with shifting community composition and environmental conditions. Our study suggests that bottom-up estimates of soil greenhouse gas fluxes can be refined by including fine-scale data on topography and tree species, enabling landscape-level estimation of GHG fluxes. Not accounting for this variation could bias our predictions for the contribution of forests to global GHG emissions and climate change. However, the bias appears to be small, at least in our study site.

ACKNOWLEDGEMENTS

We thank the field crews who collected tree census data. Research was supported by NSF awards DEB-1831952 and 1546686 to the Luquillo LTER.

REFERENCES

- Baddeley AJ, Rubak E, Turner R. 2015. *Spatial Point Patterns: Methodology and Applications with R*. London Chapman Hall: CRC Press.
- Bond-Lamberty B, Thomson A. 2010. A global database of soil respiration data. *Biogeosciences* 7:1915–1926.
- Bouskill NJ, Wood TE, Baran R, Hao Z, Ye Z, Bowen BP, Lim HC, Nico PS, Holman HY, Gilbert B, Silver WL, Northern TR, Brodie EL. 2016. Belowground response to drought in a tropical forest soil. II. Change in microbial function impacts carbon composition. *Front Microbiol* 7:1–14.
- Bouwman AF, Van Der Hoek KW, Olivier JGJ. 1995. Uncertainties in the global source distribution of nitrous oxide. *J Geophys Res* 100:2785–2800.

- Breuer L, Papen H, Butterbach-Bahl K. 2000. N₂O emission from tropical forest soils of Australia. *Journal of Geophysical Research-Atmospheres* 105:26353–26367.
- Butterbach-Bahl K, Kock M, Willibald G, Hewett B, Buhagiar S, Papen H, Kiese R. 2004. Temporal variations of fluxes of NO, NO₂, N₂O, CO₂, and CH₄ in a tropical rain forest ecosystem. *Global Biogeochemical Cycles* 18.
- Chadwick KD, Asner GP. 2016. Tropical soil nutrient distributions determined by biotic and hillslope processes. *Biogeochemistry* 127:273–289.
- Cleveland CC, Townsend AR. 2006. Nutrient additions to a tropical rain forest drive substantial soil carbon dioxide losses to the atmosphere. *Proc Natl Acad Sci* 103:10316–21. <https://doi.org/10.1073/pnas.0600989103>
- Cleveland CC, Wieder WR, Reed SC, Townsend AR. 2010. Experimental drought in a tropical rain forest increases soil carbon dioxide losses to the atmosphere. *Ecology* 91:2313–2323.
- Condit R. 1998. Tropical forest census plots: methods and results from Barro Colorado Island, Panama, and a comparison with other plots. Berlin, Germany: Springer-Verlag.
- Condit R. 2000. Spatial Patterns in the Distribution of Tropical Tree Species. *Science* (80-) 288:1414–8. <https://doi.org/10.1126/science.288.5470.1414>
- Cook BD, Corp LA, Nelson RF, Middleton EM, Morton DC, McCorkel JT, Masek JG, Ranson KJ, Ly V, Montesano PM. 2013. NASA goddard's LiDAR, hyperspectral and thermal (G-LiHT) airborne imager. *Remote Sens* 5:4045–4066.
- Courtois EA, Stahl C, Van den Berge J, Bréchet L, Van Langenhove L, Richter A, Urbina I, Soong JL, Peñuelas J, Janssens IA. 2018. Spatial Variation of Soil CO₂, CH₄ and N₂O Fluxes Across Topographical Positions in Tropical Forests of the Guiana Shield. *Ecosystems* 21:1445–1458.
- Curry CL. 2007. Modeling the soil consumption at atmospheric methane at the global scale. *Global Biogeochem Cycles* 21:1–15.
- Davidson EA, Keller M, Erickson HE, Verchot LV, Veldkamp E. 2000. Testing a conceptual model of soil emissions of nitrous and nitric oxides. *Bioscience* 50:667–680.
- Daws MI, Mullins CE, Burslem DFRP, Paton SR, Dalling JW. 2002. Topographic position affects the water regime in a semideciduous tropical forest in Panamá. *Plant Soil* 238:79–89. <https://doi.org/10.1023/A:1014289930621>
- Dwyer LM, Merriam G. 1981. Influence of Topographic Heterogeneity on Deciduous Litter Decomposition. *Oikos* 37:228–237.
- Engelbrecht BMJ, Comita LS, Condit R, Kursar T, a, Tyree MT, Turner BL, Hubbell SP. . 2007. Drought sensitivity shapes species distribution patterns in tropical forests. *Nature* 447:80–82.
- Epron D, Bosc A, Bonal D, Freycon V. 2006. Spatial variation of soil respiration across a topographic gradient in a tropical rain forest in French Guiana. *J Trop Ecol* 22:565–574.
- Erickson HE, Ayala G. 2004. Hurricane-induced nitrous oxide fluxes from a wet tropical forest. *Glob Chang Biol* 10:1155–1162.
- Groffman PM, Butterbach-Bahl K, Fulweiler RW, Gold AJ, Morse JL, Stander EK, Tague C, Tonitto C, Vidon P. 2009. Challenges to incorporating spatially and temporally explicit phenomena (hotspots and hot moments) in denitrification models. *Biogeochemistry* 93:49–77. <https://doi.org/10.1007/s10533-008-9277-5>
- Hall SJ, McDowell WH, Silver WL. 2013. When Wet Gets Wetter: Decoupling of Moisture, Redox Biogeochemistry, and Greenhouse Gas Fluxes in a Humid Tropical Forest Soil. *Ecosystems* 16:576–589.
- Hättenschwiler S, Aeschlimann B, Coûteaux MM, Roy J, Bonal D. 2008. High variation in foliage and leaf litter chemistry among 45 tree species of a neotropical rainforest community. *New Phytol* 179:165–175.
- Heartsill-Scalley T, Scatena FN, Estrada C, McDowell WH, Lugo AE. 2007. Disturbance and long-term patterns of rainfall and throughfall nutrient fluxes in a subtropical wet forest in Puerto Rico. *J Hydrol* 333:472–485.
- Holwerda F, Scatena FN, Bruijnzeel LA. 2006. Throughfall in a Puerto Rican lower montane rain forest: A comparison of sampling strategies. *J Hydrol* 327:592–602.
- Hurst MD, Mudd SM, Walcott R, Attal M, Yoo K. 2012. Using hilltop curvature to derive the spatial distribution of erosion rates. *J Geophys Res Earth Surf* 117. <https://doi.org/10.1029/2011JF002057>
- John R, Dalling JW, Harms KE, Yavitt JB, Stallard RF, Mirabello M, Hubbell SP, Valencia R, Navarrete H, Vallejo M, Foster RB. 2007. Soil nutrients influence spatial distributions of tropical tree species. *PNAS* 104:864–9. <http://www.pubmedcentral.nih.gov/articlerender.fcgi?artid=1783405&tool=pmcentrez&rendertype=abstract>
- Johnston MH. 1992. Soil-Vegetation Relationships in a Tabonuco Forest Community in the Luquillo Mountains of Puerto Rico. *J Trop Ecol* 8:253–263.
- Kaiser KE, McGlynn BL, Dore JE. 2018. Landscape analysis of soil methane flux across complex terrain. *Biogeosciences* 15:3143–3167.
- Keller AB, Reed SC, Townsend AR, Cleveland CC. 2013. Effects of canopy tree species on belowground biogeochemistry in a lowland wet tropical forest. *Soil Biol Biochem* 58:61–69. <https://doi.org/10.1016/j.soilbio.2012.10.041>.
- Kiese R, Hewett B, Graham A, Butterbach-Bahl K. 2003. Seasonal variability of N₂O emissions and CH₄ uptake by tropical rainforest soils of Queensland, Australia. *Global Biogeochem Cycles* 17:1–13.
- Liptzin D, Silver WL, Detto M. 2011. Temporal Dynamics in Soil Oxygen and Greenhouse Gases in Two Humid Tropical Forests. *Ecosystems* 14:171–182.
- Martin JG, Bolstad PV. 2009. Variation of soil respiration at three spatial scales: Components within measurements, intra-site variation and patterns on the landscape. *Soil Biol Biochem* 41:530–543. <https://doi.org/10.1016/j.soilbio.2008.12.012>.
- McSwiney CP, McDowell WH, Keller M. 2001. Distribution of nitrous oxide and regulators of its production across a tropical rainforest catena in the Luquillo Experimental Forest, Puerto Rico. *Biogeochemistry* 56:265–286.
- Min E, Wilcots ME, Naeem S, Gough L, McLaren JR, Rowe RJ, Rastetter EB, Boelman NT, Griffin KL. 2021. Herbivore absence can shift dry heath tundra from carbon source to sink during peak growing season. *Environmental Research Letters* 16.
- Muscarella R, Emilio T, Phillips OL, Lewis SL, Slik F, Baker WJ, Couvreur TLP, Eiserhardt WL, Svenning JC, Affum-Baffoe K, Aiba SI, de Almeida EC, de Almeida SS, de Oliveira EA, Álvarez-Dávila E, Alves LF, Alvez-Valles CM, Carvalho FA, Guarín FA, Andrade A, Aragão LEOC, Murakami AA, Arroyo L, Ashton PS, Corredor GAA, Baker TR, de Camargo PB, Barlow J, Bastin JF, Bengone NN, Berenguer E, Berry N, Blanc L, Böhning-Gaese K, Bonal D, Bongers F, Bradford M,

- Brambach F, Brearley FQ, Brewer SW, Camargo JLC, Campbell DG, Castilho CV, Castro W, Catchpole D, Cerón Martínez CE, Chen S, Chhang P, Cho P, Chutipong W, Clark C, Collins M, Comiskey JA, Medina MNC, Costa FRC, Culmsee H, David-Higuita H, Davidar P, del Aguila-Pasquel J, Derroire G, Di Fiore A, Van Do T, Doucet JL, Dourdain A, Drake DR, Ensslin A, Erwin T, Ewango CEN, Ewers RM, Fauset S, Feldpausch TR, Ferreira J, Ferreira LV, Fischer M, Franklin J, Fredriksson GM, Gillespie TW, Gilpin M, Gonmadje C, Gunatilleke AUN, Hakeem KR, Hall JS, Hamer KC, Harris DJ, Harrison RD, Hector A, Hemp A, Herault B, Pizango CGH, Coronado ENH, Hubau W, Hussain MS, Ibrahim FH, Imai N, Joly CA, Joseph S, Anitha K, Kartawinata K, et al. 2020. The global abundance of tree palms. *Glob Ecol Biogeogr* 29:1495–1514.
- Muscarella R, Uriarte M, Erickson DL, Swenson NG, Kress WJ, Zimmerman JK. 2016. Variation of Tropical Forest Assembly Processes Across Regional Environmental Gradients. *Perspect Plant Ecol Evol Syst* 23:52–62. <http://linkinghub.elsevier.com/retrieve/pii/S1433831916300993>
- O'Connell CS, Ruan L, Silver WL. 2018. Drought drives rapid shifts in tropical rainforest soil biogeochemistry and greenhouse gas emissions. *Nat Commun* 9:1348. <https://doi.org/10.1038/s41467-018-03352-3>.
- Osborne BB, Nasto MK, Asner GP, Christopher S, Cleveland CC, Sullivan BW, Taylor PG, Townsend AR, Porder S. 2017. Climate, Topography, and Canopy Chemistry Exert Hierarchical Control Over Soil N Cycling in a Neotropical Lowland Forest. *Ecosystems*. <https://doi.org/10.1007/s10021-016-0095-7>
- Palta MM, Ehrenfeld JG, Groffman PM. 2014. "Hotspots" and "Hot Moments" of Denitrification in Urban Brownfield Wetlands. *Ecosystems* 17:1121–37. <https://doi.org/10.1007/s10021-014-9778-0>
- Parkin TB, Venterea RT, Hargreaves SK. 2012. Calculating the Detection Limits of Chamber-based Soil Greenhouse Gas Flux Measurements. *J Environ Qual* 41:705. <https://www.agronomy.org/publications/jeq/abstracts/41/3/705>
- Plummer M. 2011. JAGS: A program for analysis of Bayesian graphical models using Gibbs sampling.
- Powers JS, Kalicin MH, Newman ME. 2004. Tree species do not influence local soil chemistry in a species-rich Costa Rica rain forest. *J Trop Ecol* 20:587–590.
- R CT. 2018. R: A language and environment for statistical computing. <https://www.r-project.org/>.
- Reed SC, Cleveland CC, Townsend AR. 2008. Tree species control rates of free-living nitrogen fixation in a tropical rain forest. *Ecology* 89:2924–2934.
- Sandel B, Svenning JC. 2013. Human impacts drive a global topographic signature in tree cover. *Nat Commun* 4:1–7. <https://doi.org/10.1038/ncomms3474>.
- Schimel JP. 2018. Life in Dry Soils: Effects of Drought on Soil Microbial Communities and Processes. *Annu Rev Ecol Evol Syst* 49:409–32. <https://doi.org/10.1146/annurev-ecolsys-110617-062614>
- Schlesinger WH. 2013. An estimate of the global sink for nitrous oxide in soils. *Global Change Biology* 19:2929–2931.
- Silver WL, Lugo AE, Keller M. 1999. Soil oxygen availability and biogeochemistry along rainfall and topographic gradients in upland wet tropical forest soils. *Biogeochemistry* 44:301–328.
- Solomon S, Qin D, Manning M, Alley RB, Bernsten T, Bindoff NL, Chen Z, Chidthaisong A, Gregory JM, Hegerl GC, Heimann M, Hewitson B, Hoskins BJ, Joos F, Jouzel J, Kattsov V, Lohmann U, Matsuno T, Molina M, Nicholls N, Overpeck J, Raga G, Ramaswamy V, Ren J, Rusticucci M, Somerville R, Stocker TF, Whetton P, Wood RA, Wratt D. 2007. Technical Summary. In: *Climate Change 2007: The Physical Science Basis. Contribution of Working Group I to the Fourth Assessment Report of the Intergovernmental Panel on Climate Change.* (Solomon S, Qin D, Manning M, Chen Z, Marquis M, Averyt KB, Tignor M, Miller HL, editors.). Cambridge University Press, Cambridge, United Kingdom and New York, NY, USA. <https://www.ipcc.ch/pdf/assessment-report/ar4/wg1/ar4-wg1-ts.pdf>
- Spiegelhalter DJ, Best NG, Carlin BP, Van der Linde A. 2014. The deviance information criterion: 12 years on. *J R Stat Soc Ser B Stat Methodol* 76:485–493.
- Tang C, Uriarte M, Morton D, Zheng T. 2021. Large-scale, image-based tree inventories in a tropical forest using artificial perceptual learning Methods in Ecology and Evolution 12: 608–618.
- Tateno R, Takeda H. 2003. Forest structure and tree species distribution in relation to topography-mediated heterogeneity of soil nitrogen and light at the forest floor. *Ecol Res* 18:559–571.
- Thompson J, Brokaw N, Zimmerman JK, Waide RB, Everham EM, Lodge DJ, Taylor CM, García-Montiel D, Fluet M. 2002. Land Use History, Environment, and Tree Composition in a Tropical Forest. *Ecol Appl* 12:1344–1363.
- Uriarte M, Turner BL, Thompson J, Zimmerman JK. 2015. Linking spatial patterns of leaf litterfall and soil nutrients in a tropical forest: a neighborhood approach. *Ecol Appl* 25:2022–34. <https://doi.org/10.1890/15-0112.1>
- Uriarte M, Muscarella R, Zimmerman JK. 2018. Environmental heterogeneity and biotic interactions mediate climate impacts on tropical forest regeneration. *Glob Chang Biol* 24:e692–e704.
- Vargas R. 2012. How a hurricane disturbance influences extreme CO₂ fluxes and variance in a tropical forest. *Environ Res Lett* 7.
- Verchot LV, Davidson EA, Cattânio JH, Ackerman IL. 2000. Land-use change and biogeochemical controls of methane fluxes in soils of eastern Amazonia. *Ecosystems* 3:41–56.
- Vidon P, Marchese S, Welsh M, McMillan S. 2015. Short-term spatial and temporal variability in greenhouse gas fluxes in riparian zones. *Environ Monit Assess* 187.
- Waring BG, Álvarez-Cansino L, Barry KEK, Becklund KK, Dale S, Gei MG, Keller AB, Lopez OR, Markesteijn L, Mangan S, Riggs CE, Rodriguez-Ronderos ME, Segnitz RM, Schnitzer SA, Powers JS. 2015. Pervasive and strong effects of plants on soil chemistry: a meta-analysis of individual plant 'Zinke' effects. *Proc R Soc B* 282:20151001.
- Wolf J, Brocard G, Willenbring J, Porder S, Uriarte M. 2016. Abrupt Change in Forest Height along a Tropical Elevation Gradient Detected Using Airborne Lidar. *Remote Sens* 8:864. <http://www.mdpi.com/2072-4292/8/10/864>
- Wolf K, Flessa H, Veldkamp E. 2012. Atmospheric methane uptake by tropical montane forest soils and the contribution of organic layers. *Biogeochemistry* 111:469–483.
- Wood TE, Detto M, Silver WL. 2013. Sensitivity of Soil Respiration to Variability in Soil Moisture and Temperature in a Humid Tropical Forest. 8:e80965.
- Wood TE, Silver WL. 2012. Strong spatial variability in trace gas dynamics following experimental drought in a humid tropical forest. *Global Biogeochem Cycles* 26:1–12.
- Zinke PJ. 1962. The Pattern of Influence of Individual Forest Trees on Soil Properties. *Ecology* 43:130–133.